TELKOMNIKA, Vol.10, No.4, December 2012, pp. 715~714
ISSN: 1693-6930
accredited by DGHE (DIKTI), Decree No: 51/Dikti/Kep/2010

Optimum Design of a Five-phase Permanent Magnet Synchronous Motor for Underwater Vehicles by use of Particle Swarm Optimization

Reza Ilka, S. Asghar Gholamian
Faculty of Electrical and Computer Engineering, Babol University of Technology, Iran
e-mail: Ilka@stu.nit.ac.ir

Abstrak

Motor sinkron magnet permanen adalah motor efisien yang memiliki aplikasi luas pada industri listrik. Salah satu aplikasi yang menarik dari motor tersebut adalah kendaraan bawah air. Pada kasus ini, perhatian utama adalah pencapaian volume minimum dan torsi tinggi. Optimasi desain dapat meningkatkan kemampuan sehingga mengurangi volume dan meningkatkan kinerja motor. Pada makalah ini, sebuah metode baru untuk desain optimum dari lima fase surface-mount motor sinkron magnet permanen disajikan untuk mencapai kerugian minimum dan volume magnet dengan peningkatan torsi. Optimasi multi-tujuan yang dilakukan dalam mencari dimensio ptimal dari motor dan magnet permanen dilakukan dengan menggunakan particle swarm optimization (PSO). Hasil desain optimasi menghasilkan sebuah motor dengan perbaikan yang tinggi terhadap motor asli. Analisis elemen hingga digunakan untuk memvalidasi keakuratan desain.

Kata kunci*: analisis elemen hingga, kendaraan bawah air*, *magnet permanen, particle swarm optimization*

Abstract

Permanent magnet synchronous motors are efficient motors which have widespread applications in electric industry due to their noticeable features. One of the interesting applications of such motors is in underwater vehicles. In these cases, reaching to minimum volume and high torque of the motor are the major concern. Design optimization can enhance their merits considerably, thus reduce volume and improve performance of motors. In this paper, a new method for optimum design of a five-phase surface-mounted permanent magnet synchronous motor is presented to achieve minimum loss and magnet volume with an increased torque. A multi-objective optimization is performed in search for optimum dimensions of the motor and its permanent magnets using particle swarm optimization. The design optimization results in a motor with great improvement regarding the original motor. Finally, finite element analysis is utilized to validate the accuracy of the design.

Keywords*: finite element analysis, particle swarm optimization, permanent magnet, underwater vehicles*

1. Introduction

Permanent magnet synchronous motors (PMSM) are one of the most proper and efficient motors in electricity industry which are good candidate for applications such as naval and space systems, electric vehicles and etc. Replacing excitation winding of rotor with permanent magnets (PM) makes these motors more efficient than their excited counterparts; hence they are used in applications with high efficiency. The most important advantages of such motors are: high efficiency and power density, low loss, low maintenance cost and etc.

One of the most interesting applications of PMSMs is to use as unmanned underwater vehicles. Due to low space and limited capacity of batteries, having maximum efficiency and minimum volume is of great concern in such systems. Hence, design optimization can enhance operational characteristics of motors. There is great number of researches in literature dealing with optimum design of PMSMs. For example, Jannot et al. [1] have presented a multiphysic modeling of a high speed PMSM which is carried out with genetic algorithm optimization. Objective functions of this paper are efficiency and weight of motor. A design optimization of PMSM forhigh torque capability and low magnet volume has been presented in [2]. In this paper, objective function is a combination of torque and magnet volume. Roshandel et al. [3] have proposed an optimization task for linear PMSM which is based on a reduction in thrust

Received June 7, 2012; Revised September 2, 2012; Accepted September 11, 2012

ripple. Design optimization of a linear permanent magnet synchronous motor for extra low force pulsations is presented in Ref. [4]. Besides, there are publications specified to design, analyze and study the PMSMs [5-9]. However, no specific research has been carried out for optimization of PMSMs in such applications.

Aim of this paper is to optimize a five-phase PMSM with surface-mounted magnet as propeller of an unmanned underwater vehicle. For this purpose, particle swarm optimization (PSO) is applied which is a new optimization algorithm. Optimization is performed with an objective function which is a combination of efficiency, magnet volume and torque of the motor.

2. Brief Description about Underwater Vehicles

Underwater vehicles (UVs) can be divided into two groups: manned and unmanned, commonly known as underwater robotic vehicles (URVs). URVs are very attractive and appropriate for operation in unstructured and hazardous environments such as the ocean, hydro power plant reservoirs and at nuclear plants.

Depending on the depth of submersion and time of autonomous operation, the mass of payload is only from 0.15 to 0.3 of the mass of vehicle. The major part of an autonomous UV's displacement is taken by the battery. The time of autonomous operation depends on the battery capacity. The motor's efficiency is very important. There are two duty cycles of UVs: continuous duty limited by the capacity of battery (up to a few hours) and short time duty (up to2 to 3 minutes). The output power of electric motors for propulsion is up to 75 kW for manned UVs (on average 20 kW) and 200 W to 1.1 kW for unmanned URVs. To obtain minimum mass and maximum efficiency the angular speed is usually from 200 to 600 rad/s [10], [11].

This paper deals with the optimum design of a five-phase surface-mounted PMSM as the propeller of an unmanned underwater vehicle (Figure 1). A 3D view of a typical surface-mounted PMSM is shown in Figure 2. Appendix A illustrates the selected specifications of a typical PMSM used for comparing to the optimized motor. These ratings and parameters are chosen according to the need of the propeller of an unmanned underwater vehicle.

Figure 1. PMSM as engine propeller

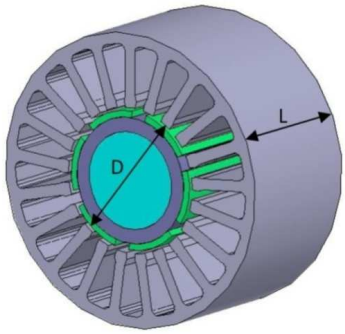

Figure 2. Typical surface-mounted PMSM

3. Machine Model

3.1. Magnetic Modelling

The air gap flux can be written as

$$\phi_g = k_l \phi = \frac{K_l}{1 + K_r \dfrac{\mu_R g A_m}{l_m A_g}} \phi_r \quad (1)$$

where l_m and A_m are the magnet length and cross-sectional area respectively, and g and A_g are the air gap length and cross-sectional area respectively. Substituting the flux concentration factor $C\Phi=A_m/A_g$, the flux density relationships $B_g=\Phi_g/A_g$ and $B_r=\Phi_r/A_m$ and the permeance coefficient as $P_c=l_m/(gC_\Phi)$ into (1) gives an air gap flux density of

$$B_g = \frac{K_l C_\phi}{1 + K_r \frac{\mu_R}{P_c}} B_r \tag{2}$$

This equation describes the air gap flux density crossing the air gap. For the motor being considered here with surface magnets, the leakage factor is typically in the range $0.9<K_l<1.0$, the reluctance factor is in the range $1.0<K_r<1.2$, and the flux concentration factor is ideally 1.0. If one considers these values to be fixed and the remanence B_r to be fixed by the magnet choice, the permeance coefficient P_c determines the amplitude of the air gap flux density. As the permeance coefficient increases, the air gap flux density approaches a maximum that is slightly less than the remanence. Without flux concentration, it is not possible to achieve an air gap flux density B_g greater than B_r Moreover, the relationship between permeance coefficient and air gap flux density is nonlinear. The air gap flux density approaches the remanence asymptotically. Doubling P_c does not double B_g. However, doubling P_c means doubling the magnet length, which doubles its volume and associated cost. The flux density in (2) defines an approximation to the air gap flux density over the surface of the magnet pole. That is, (2) gives the amplitude of the air gap flux density $|B_g|$. Over North poles (2) gives the positive amplitude and over South poles (2) gives the negative amplitude. While this approximation is far from exact, the derivation of (2) provides valuable insight into motor operation and (2) itself illustrates fundamental principles that exist even when more accurate modeling is performed [10].

The d-axis armature reaction reactance with the magnetic saturation included is

$$X_{ad} = k_{fd} X_a = 20 \mu_0 f \frac{(N_{ph} k_w)^2}{\pi P} \frac{\tau_p L}{g'} k_{fd} \tag{3}$$

where μ_0 is the magnetic permeability of free space, τ_p is pole pitch, L is the axial length of the stator core and

$$X_a = 20 \mu_0 f \frac{(N_{ph} k_w)^2}{\pi P} \frac{\tau_p L}{g'} \tag{4}$$

is the inductive reactance of the armature of a non-salient-pole (cylindrical rotor) synchronous machine. Similarly, for the q-axis

$$X_{aq} = k_{fq} X_a = 20 \mu_0 f \frac{(N_{ph} k_w)^2}{\pi P} \frac{\tau_p L}{g'_q} k_{fq} \tag{5}$$

For most PM configurations the equivalent air gap g' in equations (3) and (4) should be replaced by $gk_C k_{sat} + h_m/\mu_{rrec}$ and g'_q in eqn (5) by $gk_C k_{satq}$ where g_q is the mechanical clearance in the q-axis, k_C is the Carter's coefficient for the air gap and $k_{sat} \geq 1$ is the saturation factor of the magnetic circuit.

For salient pole rotors with electromagnetic excitation the saturation factor $k_{satq} \approx 1$, since the q-axis armature reaction fluxes, closing through the large air spaces between the poles, depend only slightly on the saturation [11].

For a salient-pole motor with electromagnetic excitation and the air gap $g \approx 0$ (fringing effects neglected), the d- and q-axis form factors of the armature reaction are

$$k_{fd} = \frac{\alpha_i \pi + \sin \alpha_i \pi}{\pi} \qquad k_{fq} = \frac{\alpha_i \pi - \sin \alpha_i \pi}{\pi} \tag{6}$$

where α_i is pole arc to pole pitch ratio.

3.2. Electrical Modelling

Total copper loss is

$$P_{cu} = 5R_s (I_s)^2 \quad (7)$$

Core loss is

$$P_c = k_h f B_m^2 + k_e f^{\ 2} B_m^2 \quad (8)$$

Mechanical loss (Windage and friction loss) is considered between 0.5 to 3 percent and stray loss is considered 0.5 to 1 percent of the output power [12], [13].

Therefore, total loss is deduced as

$$P_{Loss} = P_{cu} + P_c + P_{mech} + P_{stray} \quad (9)$$

Now, efficiency is determined through the following equation

$$\eta = \frac{P_{out}}{P_{out} + P_{loss}} \quad (10)$$

Magnet volume is defined as follow

$$V_M = \alpha_i \left(\pi(\frac{D}{2} - g)^2 - \pi(\frac{D}{2} - g - l_m)^2 \right) L \quad (11)$$

Finally, electromagnetic torque is calculated as follow [14]

$$T = \pi B_{av} L (\frac{D}{2})^2 ac \quad (12)$$

Detailed view of motor and parameters are given in Appendix B. Besides, Appendix C illustrates five-phase winding configuration of the motor designed as a case study.

4. Optimum Design with Particle Swarm Optimization

A well-known branch of meta-heuristic optimization algorithms is particle swarm optimization (PSO) which has been developed rapidly and has been applied widely since it was introduced, as it is easily understood and realized. This population-based algorithm, developed by James Kennedy and Russell Eberhart in 1995, is a stochastic search procedure based on observations of social behaviors of animals, such as bird flocking and fish schooling. In this algorithm, particles constituent population, fly through the multi-dimensional search space and each particle's velocity and position are constantly updated according to the best previous performance of the particle or of the particle's neighbors, as well as the best performance of the particles in the entire population. In this section the parameter of the BLDC motor is optimized using PSO. In the following, algorithm description is explained.

The Particle Swarm Optimization (PSO) algorithm, proposed by Kennedy and Eberhart (1995) [15], [16], inspired by social behavior of bird flocking or fish schooling. In the PSO algorithm, each solution is corresponding to a bird in the search space, considered as a particle. Each particle has a fitness value evaluated by a fitness function and a velocity in direction of particles by following present optimal particles. The algorithm is started with a random selection of particles as initial population. Particles are updated by following two values in each iteration:

First, the best fitness obtained by the particle till now (local optimum) which is saved as pbest; Second, the best fitness of all particles (global optimum) called gbest. After obtaining these two values, particles update their velocity and position:

$$V_i^{(k+1)} = w.V_i^k + C_1.rand_1(...).X(pbest_i - s_i^k) + C_2.rand_2(...).X(gbest - s_i^k) \quad (13)$$

where V_i^k denotes the ith particle's velocity in kth iteration; w is the weighting function; Cj is weighting or learning factor; rand is a random number normally distributed between 0 and 1; s_i^k is the present position of ith particle in kth iteration; pbest is the best position of ith particle while gbest is attributed to the group. The value of weighting factors is usually equal to two ($C_1 = C_2 = 2$).

Weighting function, used in the equation (13), is given below:

$$w = wMax - \left[\left(wMax - wMin\right) \times iter\right] / maxiter \quad (14)$$

where wMax is final weight; maxiter is the maximum number of iterations and iter is the number of iterations by now. For updating the position:

$$S_i^{k+1} = S_i^k + V_i^{k+1} \quad (15)$$

Large value of the inertia weight w helps the global search while small value of it helps the local search.

Particle's velocity in each dimension is clamped to a maximum velocity, Vmax. The Pseudo Code of the PSO algorithm is shown in Figure 3.

```
For each particle
Initialize particle
End
Do
For each particle
Calculate the fitness value
If the fitness value is better than the best fitness in the past (pbest)
Replace this value with the previous pbest
End
Choose the particle with the best fitness value among all particles as gbest
For each particle
Calculate the particle's velocity by equation (14)
Update the particle's position by equation (15)
End
Until termination criterion is satisfied
```

Figure 3. Pseudo Code of the PSO algorithm

For the objective function, the optimum value is produced after various tunings of PSO parameters which are listed below:

S determines the size of the population.

Vmax determines the maximum change one particle can take during each iteration.

C_1, C_2 which are learning factors and usually are equals.

Iteration which determines the maximum number of iterations the PSO execute.

From the results it can be seen that the most efficient parameter values in terms of goal functions' optimum values, convergence of optimization process, and smoothness of output plot are as Table 1.

Table1. PSO parameters values

PSO parameters	value
S	1500
Vmax	[0.001,0.01,0.01,0.005]
C_1,C_2	2
Iteration	500

The effect of each parameter listed above on the output result is described as follow. Population size (S) should be large enough to ensure convergence and smoothness of the output plot while it's too large amount is redundant. Maximum velocity (Vmax) should be small enough to ensure that the particles would not pass optimum value while it should be large enough to prevent to fall in local optima. Learning factors (C1, C2) which are usually equals and range from [0, 4].Iteration number (iteration) should be large enough to ensure the convergence while it's too large amount is redundant.

In this paper, objective function is a combination of total loss, volume of the magnets and torque of the motor. Objective function is defined as

$$F = \frac{P_{Loss}(D,L) + V_m(D,L,l_m,\alpha_i)}{T(D,L)} \quad (16)$$

that is to be minimized. This means minimizing total loss and PM volume while maximizing torque, simultaneously. In this survey, design variables are: L, D, l_m and α_i. Figure 4 shows objective function versus iteration. As shown in this figure, objective function converges and reaches to its optimal value i.e. 1.932 after 293 iterations. The optimum values of the design variables are listed in Table 2. Comparing these results with the specifications of a typical motor presented in the Appendix A shows that the design optimization results in magnets with decreased length but pole arc to pole pitch ratio slightly increased. Moreover, D has increased and L decreased.

Table 3 compares the motor parameters, d-axis and q-axis reactance, torque, PM volume and efficiency of the two designs. It can be seen that the optimization reduces the PM volume by 15.3% and increases the torque by 13% while both X_d and X_q increase. Besides, it is shown that efficiency slightly decreased. However, this reduction in efficiency is not too important and it doesn't affect the operational performance of motor. Generally speaking, this optimization provides considerable advantages for the optimized motor over the typical one in terms of initial cost, volume and performance. Different tuning in variables constraints would avoid reduction in efficiency, but on that condition torque could not be increased too high.

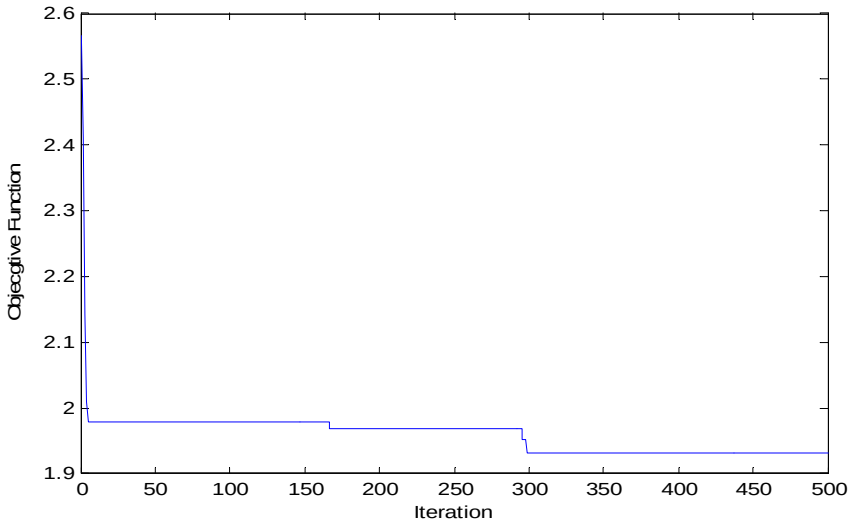

Figure 4. Objective function versus iteration

Table 2. Optimal values of design variables

Dimension/Parameter	Value
D (mm)	75
L (mm)	60
l_m (mm)	0.55
α_i	0.8

Table 3. Motor specifications

	X_d (Ω)	X_q (Ω)	V_m (cm^3)	T (Nm)	Efficiency (%)
Typical motor	23.05	21.02	7.57	3.36	89.26
Optimized motor	25.53	24.3	6.41	3.7968	89.009

5. Finite Element Analysis Validation

The design optimization in this paper is totally based on analytical models of motor presented. Therefore, the accuracy of the electrical and magnetic models validates the design optimization. In this section, finite element analysis (FEA) is used for validation. Maxwell software which is based on FEA is one of the most important and efficient tools for this purpose.

We give the software the dimensions obtained by optimization. A 2D FEA is carried out and the numerical and graphical results are obtained. Figure 5 shows flux lines diagram and Figure 6 shows voltage and current of one phase of motor. As shown in this Figure 6, RMS value of phase voltage and phase current is close to the rated values of motor. Also, moving torque of motor is shown in Figure 7. This torque value has a minimum deviation with the one obtained by analytical design. Table 4 presents a comparison between results of analytical optimization and finite element analysis.

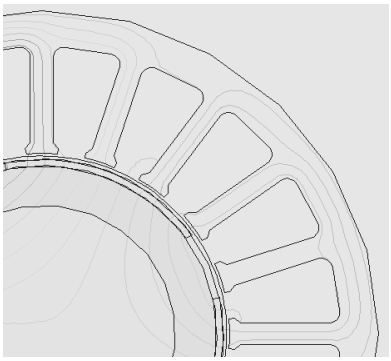

Figure 5. Flux lines diagram

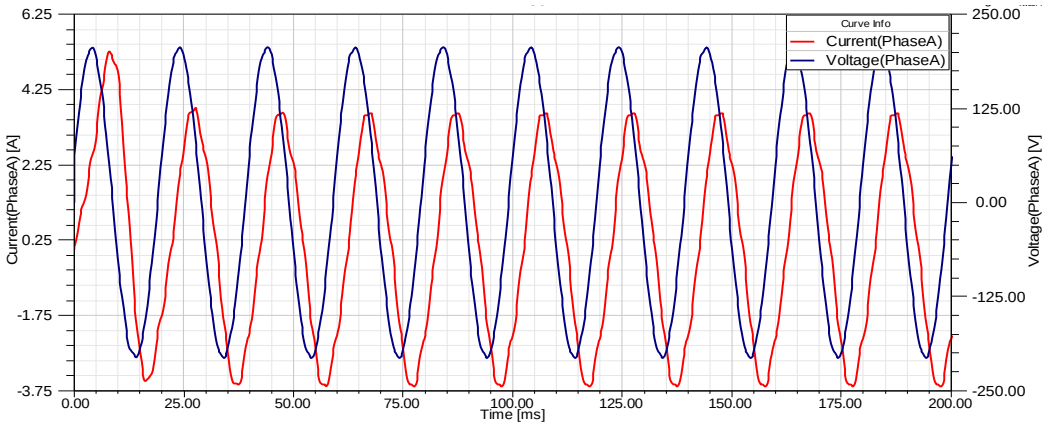

Figure 6. Voltage and current of phase A

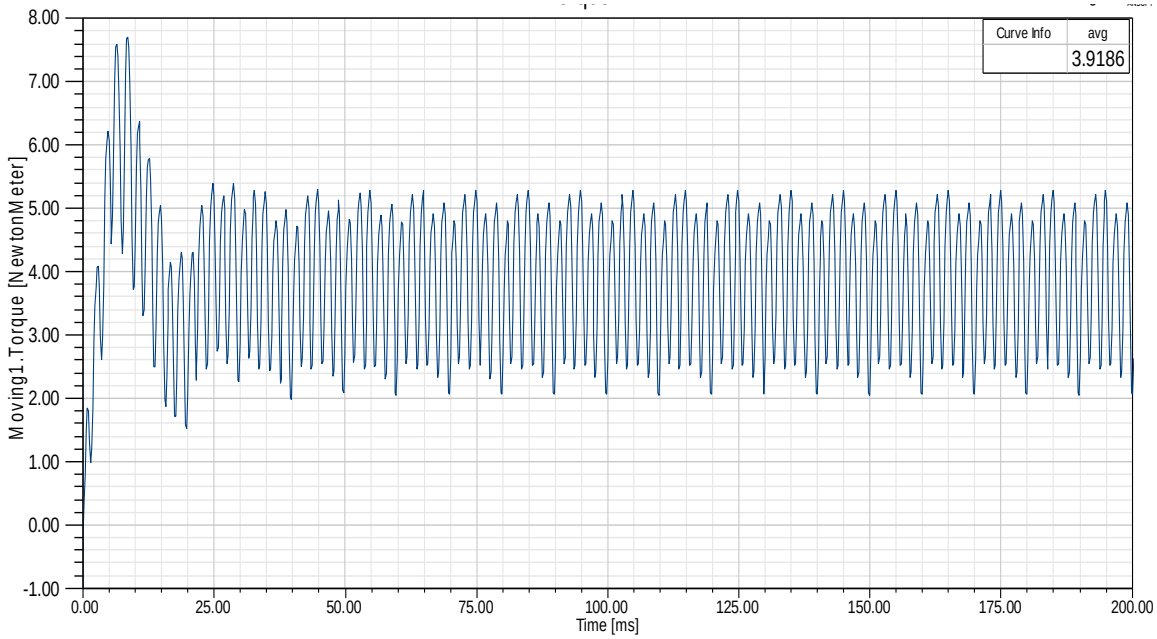

Figure 7. Moving torque of motor

Table 4. Comparison of analytical optimization and FEA results

Results	Analytical models	FEA	Error (%)
X_d (Ω)	25.53	23.257	8.9
X_q (Ω)	24.3	22.43	7.6
T (Nm)	3.72	3.9186	5.3
Efficiency (%)	89.009	90.68	1.8

6. Conclusion

This paper presented an optimum design for a five-phase surface-mounted permanent magnet synchronous motor. Design optimization is performed in search for proper dimensions of motor and its magnets to achieve a reduced total loss and magnet volume and a high torque. The design optimization leads to a motor with more than 15.3% reduction in magnet volume and 13% increase in the torque with respect to the original motor. Finally, finite element analysis confirmed the analytical design with minimum error which proves the efficiency and accuracy of the design.

Future works may be devoted to optimization of such motors with other optimizing algorithms or other objective functions.

References

[1] X Jannot, J Vannier, C Marchand, M Gabsi, J Saint-Michel, D Sa. Multiphysic Modeling of a High-Speed Interior Permanent Magnet Synchronous Machine for a Multiobjective Optimal Design.*IEEE Transactions on Energy Conversion*.2011; 26(2).

[2] S Vaez-Zadeh, AR Ghasemi. Design Optimization of Permanent Magnet Synchronous Motors for High Torque Capability and Low Magnet Volume.*Electric Power Systems Research.* 2005; 74: 307–313.

[3] N Roshandel Tavana, A Shoulaie. Pole-shape Optimization of Permanent-magnet Linear Synchronous Motor for Reduction of Thrust Ripple.*Energy Conversion and Management.*2011; 52: 349–354.

[4] A Hassanpour Isfahani, S Vaez-Zadeh. Design Optimization of a Linear Permanent Magnet Synchronous Motor for Extra Low Force Pulsations.*Energy Conversion and Management.*2007; 48: 443–449.

[5] L Parsa, HA Toliyat, A Goodarzi. Five-Phase Interior Permanent-Magnet Motors with Low Torque Pulsation.*IEEE Transactions on Industry Applications*. 2007; 43(1).

[6] MS Islam, R Islam, T Sebastian. Experimental Verification of Design Techniques of Permanent-Magnet Synchronous Motors for Low-Torque-Ripple Applications.*IEEE Transactions on Industry Applications*.2011; 47(1).
[7] Y Li, J Xing, T Wang, Y Lu. Programmable Design of Magnet Shape for Permanent-Magnet Synchronous Motors With Sinusoidal Back EMF Waveforms.*IEEE Transactions on Magnetics*. 2008; 44(9).
[8] A Hassanpour Isfahani, S Vaez-Zadeh. Line Start Permanent Magnet Synchronous Motors: Challenges and Opportunities.*Energy.* 2009; 34: 1755–1763.
[9] N Bianchi, S Bolognani, P Frare. Design Criteria for High-Efficiency SPM Synchronous Motors.*IEEE Transactions on Energy Conversion*. 2006; 21(2).
[10] DC Hanselman. Brushless Permanent Magnet Motor Design.Magna Physics Publishing. 2nd edition, 2006.
[11] JF Gieras, M Wing.*Permanent Magnet Motor Technology: Design and Applications*. CRC Press. 2nd Edition. 2002.
[12] HA Toliyat, GB Kilman.*Handbook of Electric Motors*. CRC Press. 2nd Edition. 2004.
[13] ES Hamdi.*Design of Small Electrical Machines*. John Wiley & Sons. 1994.
[14] J Pyrhonen, T Jokinen, V Hrabovcova.Design of Rotating Electrical Machines. John Wiley & Sons. 2008.
[15] RC Eberhart, J Kennedy.*A New Optimizer Using Particle Swarm Theory*. Proceedings of the Sixth International Symposium on Micro Machine and Human Science. Nagoya, Japan, 39-43. Piscataway, NJ: IEEE Service Center. 1995.
[16] CM Yang, D Simon. *A New Particle Swarm Optimization Technique*. Proceedings of the 18th International Conference on Systems Engineering (ISCEng 2005).*IEEE Computer Society*. Washington. 2005.

Appendix A

Typical motor specifications used as a basis for comparison

Parameter	Description	Value
P_{out}	Output Power	550 W
V_n	Rated Voltage	220 V
P	Number of poles	4
n_s	Rated Speed	1500 rpm
I_s	Phase Current	1.4 A
f	Drive Frequency	50 Hz
D	Stator Inner Diameter	67.5 mm
L	Motor Axial Length	66.1 mm
D_{out}	Stator Outer Diameter	121 mm
h_{bi}	Stator yoke height	8.8 mm
h_s	Slot height	18 mm
l_m	Permanent Magnet Length	0.7 mm
α_i	Pole arc to pole pitch ratio	0.75
g	Air Gap Length	0.9 mm
B_{av}	Average flux density	0.5 T
ac	Specific electric loading	22000 A/m
B_r	Remanent flux density	1.2 T
B_s	Saturation flux density	1.5 T
τ_p	Pole Pitch	52.9 mm
K_w	Winding factor	0.95
S	Slot number	20
N_{ph}	Stator Turns per Phase	343
Z_{slot}	Number of Conductors per Slot	171
R_s	Stator Resistance per Phase	4.5 Ω

Appendix B
Dimensions and parameters of the motor

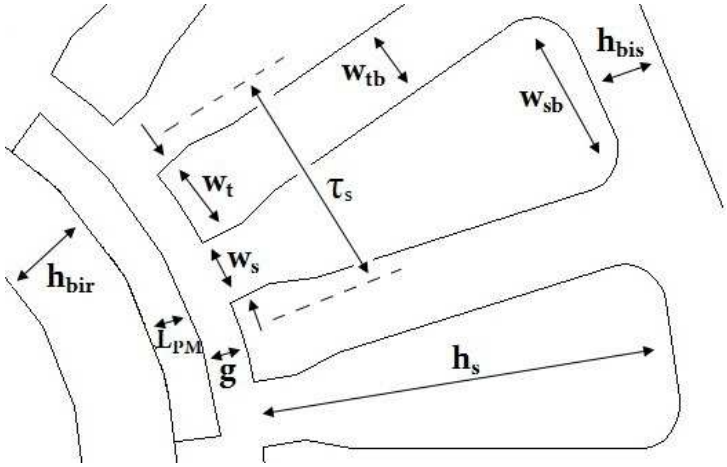

Appendix C
Five-phase winding configuration